

# Polar coordinate laser writing systems: error analysis of fabricated DOEs

Alexander Poleshchuk<sup>\*a</sup>, Victor Korolkov<sup>a</sup>, Vadim Cherkashin<sup>a</sup>, Stephan Reichelt<sup>\*\*b</sup>, Jim Burge<sup>\*\*\*c</sup>

<sup>a</sup>Institute of Automation and Electrometry, SB RAS, 630090, Novosibirsk, Russia.

<sup>b</sup>Institut für Technische Optik, Universität Stuttgart, 70569 Stuttgart, Germany

<sup>c</sup>University of Arizona, Tucson, Arizona, 85721, USA

## ABSTRACT

Diffractive optics is a field where the progress is defined by fabrication technology. Diffractive optical elements (DOEs) are generally planar structures, typically fabricated using X-Y image generators designed for semiconductor industry. However there are some kinds of DOEs for which the polar scanning geometry, where the optic rotates under a writing beam, is more preferable. In some cases polar coordinate machines provide the only practical method of fabricating DOEs with the required accuracy. It is necessary to take into account the DOE specification when choosing the fabrication method.

The present paper considers peculiarities of polar coordinate laser systems for large size and high precision DOEs fabrication. The specific error sources for these systems are described and compared with those of X-Y systems. An optimal writing strategy is discussed.

The wavefront aberrations of rotationally symmetric DOEs caused by fabrication errors were measured interferometrically. Different types of aberrations were identified and can be referred to certain writing errors. Interferometric measurements of the wavefront errors for binary zone plates with a 64 mm diameter and 0.45 numerical aperture have shown that the wavefront root-mean-square error does not exceed  $0.009\lambda$ .

Keywords: Diffractive optical elements, DOE, computer generated holograms, CGH, polar coordinate writer, fabrication errors, fabrication tolerances.

## 1. INTRODUCTION

Developments in the field of diffractive optics are limited by the technologies used to manufacture them. Conventional diffractive optical elements (DOEs) are planar structures, fabricated using X-Y laser (or e-beam) writing systems designed for the semiconductor industry. However there are several types of DOEs with axial symmetry for which the circular scanning is more suitable. Some examples are focusing optics, wavefront correctors, aspheric nulls, non-diffracting beam generators, DOE with spatial carriers of polar geometry, etc.<sup>1-3</sup>. The patterns with circular symmetry are optimally manufactured using equipment with that same symmetry. Rotation of the substrate provides one motion and radial motion of a writing head provides the other.<sup>4-12</sup>

Some computer-generated holograms used for optical testing must have the circular diffractive structure fabricated with an accuracy of no worse than  $0.1\mu\text{m}$ , a minimal period of less than  $1\mu\text{m}$ , for overall dimensions of a few hundreds of millimeters. In addition, the substrate surface must be flat to  $\lambda/20$ . This type of diffractive element can be fabricated only by means of polar coordinate writing systems. That is why, choosing a method of DOE fabrication, one must take into account the specific application of the DOEs. Accuracy of the diffractive structure manufacturing is decisive in fabricating DOEs for certifying the classical optical elements and systems<sup>12-15</sup>.

This present paper considers peculiarities of a polar coordinate laser writing system<sup>11</sup> for fabricating large and high precision DOEs. Such systems (CLWS-300 developed by joint efforts of Institute of Automation and Electrometry and

\* poleshchuk.a.g@iae.nsk.su; fax 007-3832-333-863; <http://www.iae.nsk.su>

\*\* reichelt@ito.uni-stuttgart.de; tel: 049-0711/685-6066; fax: 049-0711/685-6586; <http://www.uni-stuttgart.de/ito/>

\*\*\* JBurge@optics.Arizona.EDU; tel.: 520-621-8182

Technical Design Institute, Russia, Novosibirsk) are widely used for DOE fabrication<sup>16-18</sup>. The sources of specific errors for these and other similar systems are described and compared with those of X-Y systems. The optimal writing strategy for minimization of errors is discussed.

## 2. POLAR COORDINATE LASER WRITING SYSTEM

A schematic diagram of the laser writing system CLWS-300<sup>11</sup> is shown in Fig. 1. The system can be subdivided into four main units: the angular units (motorized air-bearing spindle and rotary encoder), the radial positioning unit (motorized air-bearing stage and interferometer), the writing power control unit (two acousto-optic modulators AOM1 and AOM2), and the optical writing head (focusing lens, autofocus sensor, reflection photodetector). All opto-mechanical units are mounted on granite base with vibration isolators.

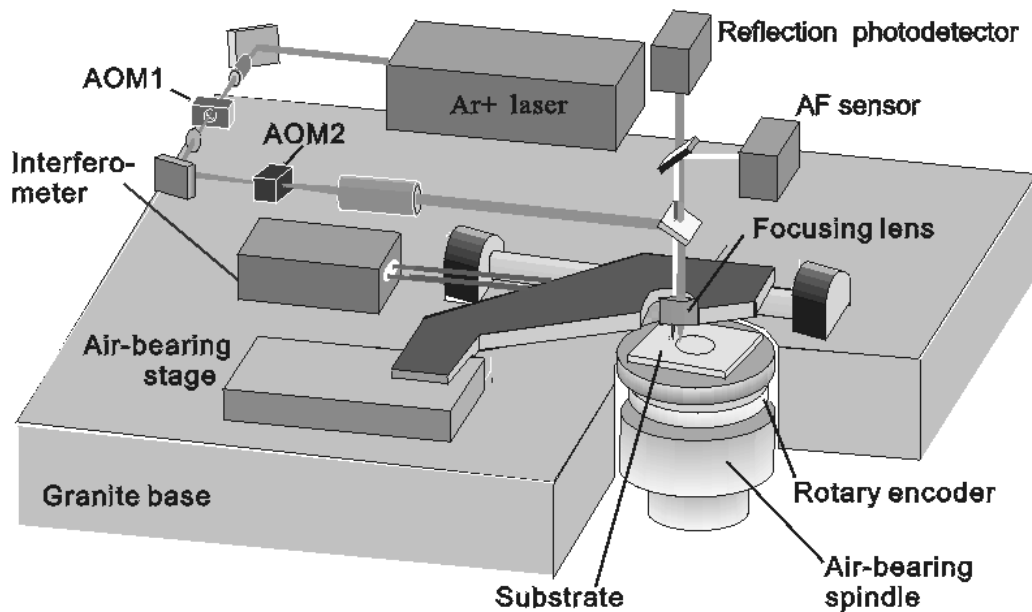


Figure 1. Schematic diagram of the polar coordinate laser writing system.

The performance and specifications of the developed laser writing system CLWS-300 are summarized in Table 1.

Table 1. Performance and specifications of the CLWS-300.

Maximum diameter of the writing field	300 mm
Substrate thickness	1.5 –30 mm
Recording spot diameter (full-width half-maximum)	0.5 $\mu\text{m}$
Rotation speed	300 - 800 rpm
Accuracy of radial coordinate positioning (RMS)	0.1 $\mu\text{m}$
Accuracy of angular coordinate measurement (RMS)	1 arc s
Wavelength of writing beam	457-514 nm (Ar <sup>+</sup> laser)
Writing time (0.5 $\mu\text{m}$ raster pitch on the field of 90 mm diameter)	about 2 hours
Writing technologies	Thermochemical writing on Cr films; gray-scale writing in LDW-glass, a-Si films; direct writing in resist films.

### 3. SPECIFIC ERROR SOURCES FOR CLWS

The task of DOE fabrication is to write binary, relief, or gray-scale structures with their area up to  $10^4 \text{ mm}^2$ , with minimal features up to  $0.5 \text{ }\mu\text{m}$ , and accuracy of  $0.05\text{-}0.1\text{ }\mu\text{m}$  over the entire surface of element. The DOE structure at writing in CLWS is represented in hybrid pixel-vector format: in radial coordinate direction the pixel representation with variable pixel size is used, and in angular direction the pattern is presented as a set of elementary vectors with origins and ends described in angular units. But for simplicity we consider only pixel representation of DOE structure. Because at binary writing only the origin and end of vectors are important, and they can be presented as pixels with coordinates  $P_i(r_i, \theta_i)$  in polar coordinate system, where  $r_i$  - is the writing radius (distance from spindle rotation axis to center of laser writing spot);  $\theta_i$  is the angular coordinate of writing spot center (defined as the distance between the angular coordinate origin ( $\theta=0$ ) and the current angular position of the spinning table). The writing process introduces errors in DOE structure. These errors have two components:

- the difference between the calculated  $P_i(r_i, \theta_i)$  and written  $P'_i(r'_i, \theta'_i)$  coordinates of  $i$ -th pixel.
- the difference in shape between the calculated and actually written pixel (size error).

The first component depends on the accuracy of laser beam displacement with respect to the substrate. The second error is caused by variations in beam power and spot size. Both these components define the position of the zone boundary. The local pattern distortion error  $\zeta$  (in direction perpendicular to the zones) in binary DOEs is defined by averaging the displacements of the inner and outer zone boundary ( $\zeta_{in}$  and  $\zeta_{out}$ ), respectively:

$$\zeta = (\zeta_{in} + \zeta_{out})/2. \quad (1)$$

Local pattern distortion error results in an additional phase shift of the wavefront of the light flux transmitted through the fabricated DOE. The phase shift or the so-called wavefront pattern distortion error  $W$  introduced by an imperfect hologram pattern can be defined as<sup>14,15</sup>

$$W = -m\lambda\zeta/p, \quad (2)$$

where  $m$  is the diffraction order,  $\lambda$  is the wavelength of light and  $p$  is the local zone period of the DOE. The total writing error of rotationally symmetric DOEs is primarily determined by the effects described below.

#### 3.1 The error of fixing the origin of coordinates

The rotation axis of the spindle must be the origin of the polar coordinate system ( $r = 0$ ) in CLWS. Still, it is a serious problem to find extremely precisely the rotation axis position. The distances  $y_0$  and  $x_0$  between the reference point of the laser interferometer and the center of substrate rotation introduce an error in the coordinate of the current exposed point<sup>14</sup>. The actual polar coordinate of the point written is  $P'_i(r'_i, \theta'_i)$ . The radius  $r' = r + \Delta r$  and the polar angle  $\theta'$  is not changed from the ideal value of  $\theta$ .

#### 3.2 Drift of coordinates origin during writing process

The machine geometry is not perfectly stable due to several effects: primarily thermal drift and expansion of mechanical parts of air-bearing spindle and interferometer, but also drift of interferometer laser wavelength. Thermal drifts depend on the environmental temperature stability and transfer of heat from the motor, electronics, and laser. These effects are minimized by running the full system for several hours to equilibrate the temperatures before writing the patterns. Drift of interferometer laser wavelength can contribute to system errors if the air temperature and pressure is not stable. Therefore the environment (temperature and pressure) must be taken into account for wavelength correction during writing process or in interferogram processing when measuring aspherical wavefront.

#### 3.3 Rotation trajectory error

The error of a spindle rotation trajectory is a deviation of the trajectory of movement of some point on the spinning table from an ideal circle. This error consists of the deviation of the spindle rotation center (eccentricity) and the angular deviation of the axis of rotation (runout of the rotation axis). The real writing coordinate will be (at  $r \gg \Delta r$ ) the following:

$$r' = r + \Delta r(\varphi), \quad (3a)$$

$$\theta' = \theta + \arctg[\Delta r(\theta - \pi/2)/r]. \quad (3b)$$

The error of rotation trajectory depends on the angular position and is due to inaccurate fabrication of the air bearing spindle parts. The typical error for a spindle on the air bearing is usually below 0.1  $\mu\text{m}$ . The form of the curve is sufficiently stable and reproducible. This kind of error leads to distortion of the writing coordinates.

### 3.4 Error of writing spot displacement in the radial direction

Any deviation from linear displacement results in a writing coordinate error. The air bearing stage displaces the focusing optics and determines the writing spot position on the substrate in the radial direction. The accuracy of stage displacement by a given coordinate depends on the transient process time, the increments and long-time stability of the interferometer, the Abbe errors, etc. The displacement of the stage is accompanied by tilting in all coordinates. The greatest error is introduced by the angular deviation  $\varphi_z$  in the plane of the spinning table, while the contribution from the other angular deviations are minimized by decreasing the lengths of consoles and using the autofocus.

## 4. EVALUATION OF ERRORS SPECIFIC FOR CLWS

### 4.1 Center searching

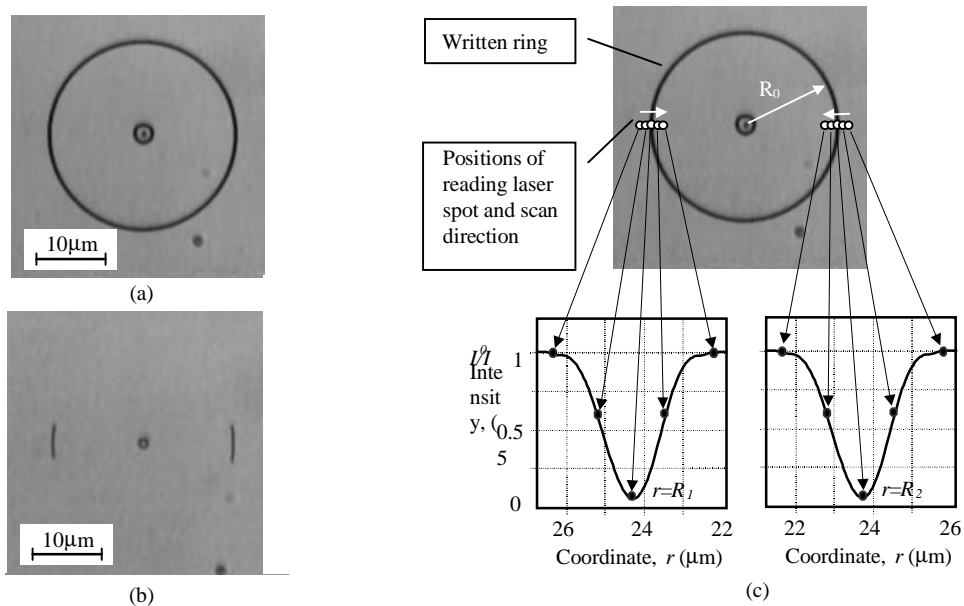


Figure 2. Examples of micrographs of center area of substrate (chromium film, 70 nm thickness,) with written ring (a) and two arcs (b). Trajectory of displacement of reading laser spot at the procedure of the center searching and typical intensity distributions of reflected light (c).

To define practically all specific for CLWS errors it is necessary to measure relative position spindle rotation axis and center of writing spot. Several methods for determining the spindle rotation axis are known<sup>7,23</sup>. As a rule, these methods are based on interchanging substrate with photosensitive media onto special sample (wedged reflecting substrate, spherical lens, grating etc.). It is difficult to use these methods during the time of DOE writing. To measure relative position of spindle rotation axis and writing spot center at the time of DOE writing it was suggested to write a small ring (diameter of 20-60  $\mu\text{m}$ ) around rotation center and to align it with the writing beam using the microscope<sup>12</sup> or photoelectrical scanning measurement<sup>14</sup>. To apply this method the substrate with a chromium film or other photosensitive coating is fixed on the spinning table of the CLWS (Figure 1). The writing laser beam is roughly positioned in the region of center (accuracy about 1-2  $\mu\text{m}$ ) and radial coordinate counter is reset. At some distance from rotation center (for example,  $R_0 = 10-50 \mu\text{m}$ ) a ring with radius  $R_0$  (see Figure 2 (a)) or two small arcs (see Figure 2 (b)), are written on the rotating substrate. Writing is carried out with three passes on the same place to provide the uniformity of the ring width (see Section 5). The values of writing power are selected experimentally for each type of the chromium film for sufficient changing the film reflection (oxidation and melting). It is very important that the center is determined using the same laser writing spot (but with dramatically

reduced power) and on the substrate which is intended for DOE fabrication. Scanning photoelectric reading is carried out using reflection photodetector (see Figure 1) in writing head of CLWS. The reading spot moves on first external radius  $r_1=R_0 + d/2$ , where  $d$  - is a scanning range and scans to center direction. A scanning trajectory of a reading laser spot and typical reflection distributions are shown in Figure 2 (c). A scanning range is usually about 3-6  $\mu\text{m}$ . Then reading spot moves on second external negative radial coordinate  $r_2= -R_0 - d/2$  and scans to center direction again. After searching the coordinates of points with minimum reflection ( $R_1$  and  $R_2$ ) the error of coordinate of rotation center is defined as  $x_0 = (R_1 - R_2)/2$ .

#### 4.2 Long term repeatability of origin coordinate position

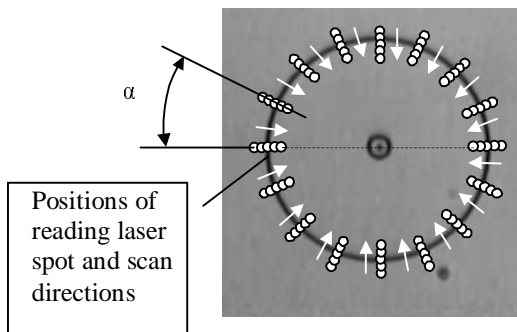


Figure 3. Measurement of rotation trajectory.

It is possible to find the center automatically at regular time intervals or radial coordinates to check for thermal drifts of the systems. For this purpose the writing process is interrupted and rotation center is determined. The current errors of coordinate origin are saved for a following mathematical processing of the interferogram of the measured asphere. Periodical correction (reset of linear coordinate) can be also used at the long writing of large DOEs. This procedure very effectively decreases an influence of thermal drift for the CLWS. To make these corrections, the writing process is periodically interrupted, and the writing head is moved to the origin of radial coordinates and the center of rotation is determined. Any motion in this from the previous value indicates an error, which is then corrected.

#### 4.3 Measurement of a rotation trajectory of a spindle

The method of a rotation trajectory measurement is based on repeated  $N$  times measurements of small ring diameter  $D_N=R_1+R_2$  (see Section 4.1) at different spindle angular positions  $\alpha=360^\circ/N$  as shown in Figure 3. Measurements can be made both with non-rotating spindle (spindle with substrate is consecutively manually turned) or automatically with rotating spindle. Real results of measurements will be discussed in Section 6.2.

### 5. WRITING STRATEGIES FOR HIGH PRECISION DOE FABRICATION

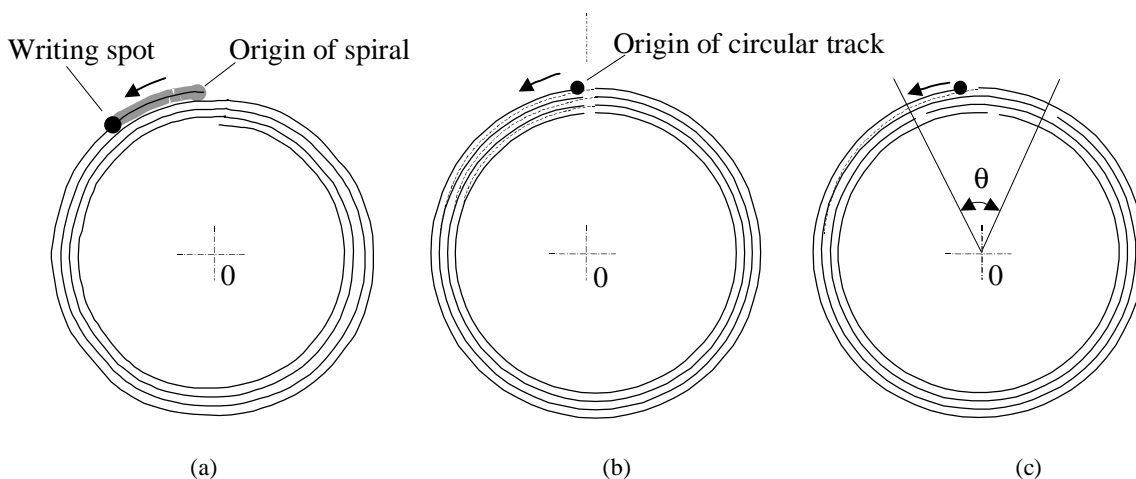


Figure 4. Methods of writings: spiral (a), circular (b) and circular with random scattering of track origin (c).

Let's consider the strategy of writing for axisymmetrical DOEs by means of CLWS ensuring maximal accuracy of manufacturing. In this case the center of DOE is aligned with spindle rotation axis. The size of circular zones of typical DOE can vary from several millimeters to less than one micron. The writing of such zones is made by repeated passes of the recording spot with overlapping. Spiral (Figure 4 (a)) or circular (Figure 4 (b)) scanning (and also their combination <sup>7</sup>) is possible. The spiral scanning provides a high speed of writing and absence of hitches at moving the linear stage. However

because of an eccentricity, this way is applied only at fabrication of inaccurate DOEs and for filling up the middle area of large zones in precision DOEs. As the quality of DOE is determined by accuracy of boundaries of its zones, it is necessary to apply circular scanning. The radial step  $\Delta r$  of circular scanning is varied on the base of requirement to fill zones symmetrically, as shown in Figure 5.

When the zone width  $L$  is equal or a little more than effective width of a recording spot  $D$ , the writing is made by three ( $N = 3$ ) circular passes with a step  $\Delta r_i = (L-D)/2$  (Figure 5 (a)). When the radial step exceeds value  $\Delta r_{max} = n \cdot D$ , where  $n = 0.5-0.8$ , the writing of zones starts with 4 passes (Figure 5 (c)). Thus the radial step for outermost passes is hold equal  $\Delta r_{max}$ , and between central passes the radial step  $S_i$  continuously varies from null up to  $\Delta r_{max}$  at further increase of width of zones. Such algorithm of changing a radial step and quantity of passes allows to simplify a procedure of choice of writing beam power depending on radial coordinate and to increase accuracy of exposing the boundaries of circular zones at the expense of a statistical average.

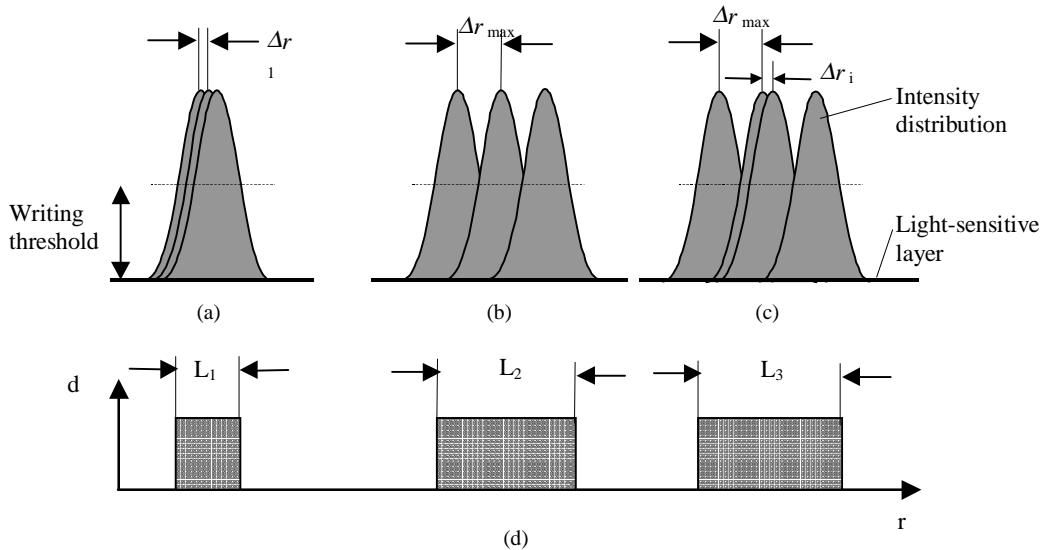


Figure 5. Method of filling zones. Intensity distributions in writing spots (a,b,c) and written zones (d).

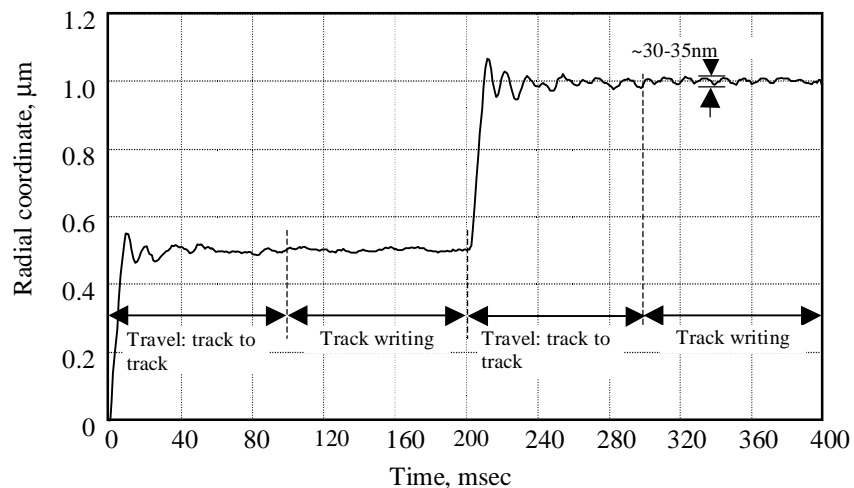


Figure 6. Typical transient process of radial positioning in CLWS.

Multi-pass writing<sup>24</sup> reduces the effect of random errors of a position of recording laser beam, vibrations of the system and transients in the linear stage. The multi-pass writing reduces throughput of the CLWS approximately proportionally to quantity of passes. However advantages of multi-pass averaging is more important for manufacturing the high-precision reference DOEs with narrow zones. Usually the multi-pass averaging provides a desirable effect only when the errors are truly random. In other cases the improvement less notable. Figure 6 depicts the segment (two passes with a step 0.5

microns) of transient process of a system of radial positioning in CLWS of IAE<sup>19</sup>. It is visible, that along with accidental errors there is a systematic oscillatory component caused by resonant phenomena. For effective smoothing of this component (which is most appreciable in the beginning of a circular track) in CLWS we utilize a random scattering of the origin of circular tracks (Figure 4 (c)). The scattering is made within the limits of a angle from 30 to 45° and eliminates also joints (ring track butting) at the beginning and end of tracks. Figure 7 demonstrates the efficiency of this method. It shows the pieces of zones of circular DOE written without scattering (a) and with scattering (b) for the track origin. It is visible, that the scattering essentially improves the characteristics of writing.

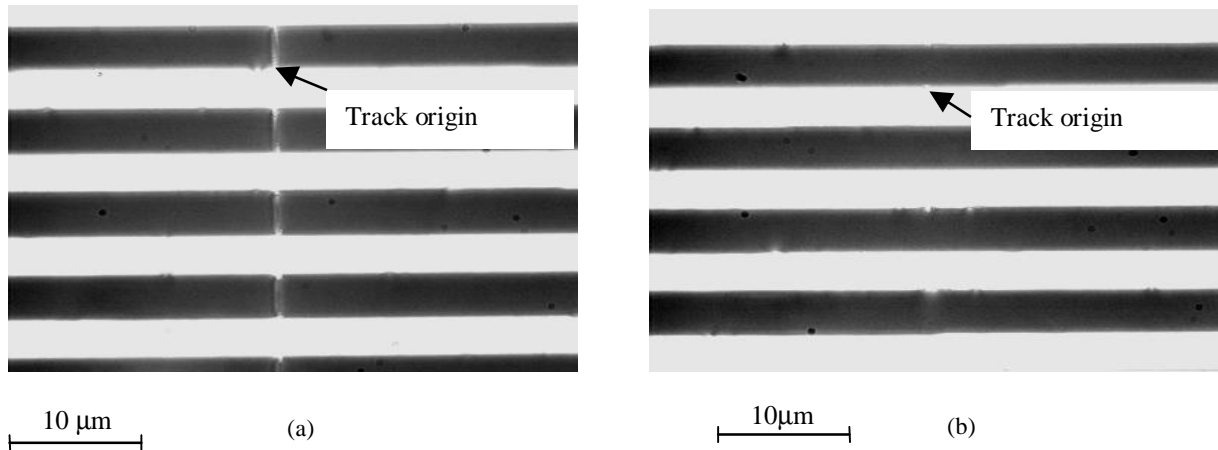


Figure 7. Fragments of zones of circular DOE written without scattering (a) and with scattering (b) of track origin.

The methods of the precision DOE writing (described in the given Section) are shown in Table 2.

Table 2. Methods of writing using CLWS

Method	Expected Result	Shortcomings
Circular scanning	Elliptically elimination	Reduce throughput by a factor 2
Many passes (N – pass) at writing of narrow zones	Zone width uniformity	Reduce throughput by a factor N
Symmetry of zone filling	Zone width uniformity	-
Scattering of circular track origins.	Angular uniformity	Reduce throughput by a factor about $\theta/360^\circ$

The majority of presented methods results in an increase of writing time of DOE. Therefore optimum strategy of writing should search for a balance between writing rate and accuracy.

## 6. SPECIFICATION OF THE PATTERN DISTORTION WAVEFRONT ERROR

Main error source of a CGH is due to pattern distortion. The wavefront error  $W_{PD}$  introduced by a CGH that includes any pattern inaccuracies is given by Eq. (2). This equation is valid for single reflection or single pass. Besides, all variables in Eq. (2) except the pattern error  $\zeta$  are well-known, since they are defined by the design of the CGH. Therefore, if the pattern error  $\zeta$  can be determined somehow, the wavefront error  $W_{PD}$  can be calculated and used for error budgeting of the hologram.

We embark on *two strategies* to characterize the pattern error  $\zeta$  that is inherent in the CGH. Firstly, to detect drifts of the radial coordinate, the above described procedure of automatic center searching during the writing process is used. The second strategy we used is a manual measurement of the spindle trajectory after writing the CGH. Here we scanned the center-near test ring again, but now the measurement is performed on the non-rotating spindle. One measurement returns the radius value in positive and in negative direction (from origin of linear coordinate). The ring is then scanned  $N$  times (see Section 4.2), whereby the spindle with the substrate is consecutively manually rotated by  $\pi/N$ .

### 6.1 Non-rotationally symmetric pattern distortion error

We observed spoke-shaped aberrations in wavefronts reconstructed from our CGHs. These aberrations result from a vibration of the air bearing spindle. The angular frequencies are dependent on the rotation speed of the machine spindle. For instance, at 600 rpm rotation speed there exists a characteristic error at angular frequencies  $8/(2\pi)$  and  $9/(2\pi)$  with amplitudes of about 60 nm and 40 nm, respectively (Figure 8).

The manual measurement of the spindle trajectory explained above is used to detect the non-rotationally writing error  $\zeta_{NRS}(\theta)$ . Applying the Fourier transform to the measured curve gives the amplitude- and phase spectrum in the frequency domain. With the amplitude- and phase distributions the pattern error  $\zeta_{NRS}(\theta)$  can be expressed as a Fourier series of cos-functions.

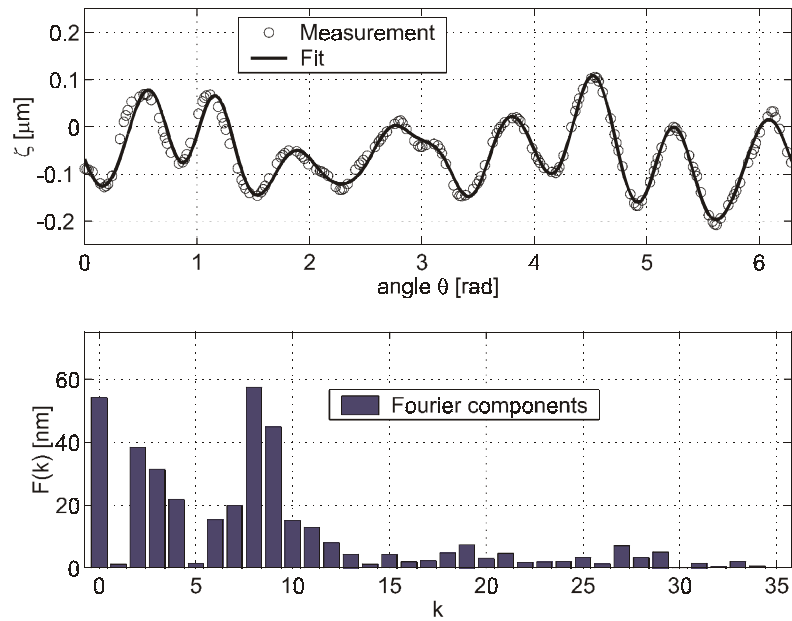


Figure 8. Systematically non-rotationally symmetric pattern distortion error  $\zeta_{NRS}$ . The upper diagram shows the result of manual measurement of spindle trajectory at a radius of 490  $\mu\text{m}$  and a Fourier fit. The lower diagram shows the amplitude spectrum of the Fourier transform of the measured trajectory. Example: non-rotationally symmetric pattern error of a  $f/3$  Fresnel zone plate.

### 6.2 Rotationally symmetric pattern distortion error

Rotationally symmetric pattern errors result from a radial displacement of zones and can be divided into a drift error  $\zeta_{CD}$  and a constant positioning error  $\zeta_{Const}$ . The former results from thermal drifts of the system and environmental changes (temperature and air pressure influence the effective refractive index of air and thus the interferometric measurement of the radial position), whereas the latter result from an faulty definition of the center.

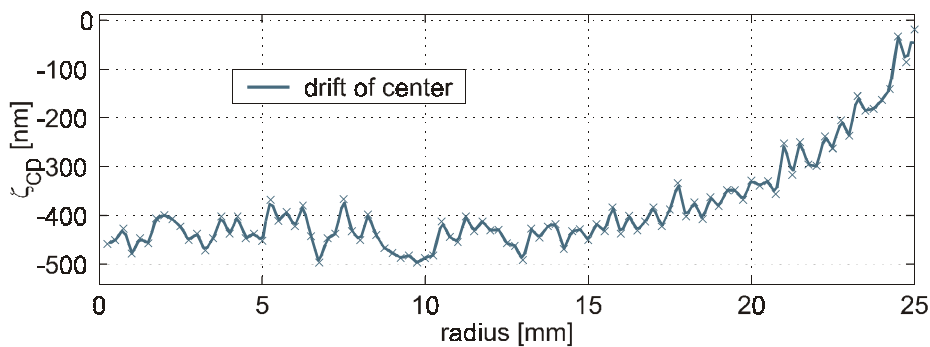


Figure 9. Example of a center drift  $\zeta_{CD}$ , monitored during the CGH writing process of a  $f/1$  Fresnel zone plate

Since the increment of the length measuring interferometer which controls the radial position of the writing laser is 79 nm (CLWS-300 before modernization), any resetting of a drift leads to a jump of at least 79 nm. However, jumps in the pattern distortion error  $\zeta$  result in high frequency wavefront errors. To avoid such high frequency errors in the CGH we only detect the center error during the writing process, without compensating its influence. In this case a smooth wavefront error results, which can be easily approximated by a set of Zernike polynomials. In Figure 9 an example of center-zero error is depicted. The amount of the constant positioning error  $\zeta_{Const}$  is obtained from the manual spindle trajectory measurement. Since the ideal radius of the test circle is known, the Fourier component for  $k = 0$  (offset) yields the deviation from it. For the constant positioning error  $\zeta_{Const}$  we obtained 54 nm for the example depicted in Figure 8.

### 6.3 Comparison between wavefront error prediction and measured wavefront error

If the pattern error was recorded during the fabrication process, the quality of the wavefront reconstructed by the CGH can be specified and used for calibration of the measuring system. Here, we estimate both error types, axially symmetric as well as the non axially symmetric with the methods described above. Inserting the pattern error  $\zeta(x,y)$  and design data (local period  $p$ ) into Eq. (2) yields the expected wavefront error due to fabrication inaccuracies of the hologram pattern. In Figure 10 an example for a predicted wavefront error  $W_{PD}$  is depicted, divided in rotationally- and non-rotationally symmetric parts.

Figure 11 shows the measured wavefront aberration of a  $f/1$  Fresnel zone plate tested at confocal position in reflection mode. The zone plate has a diameter of 50 mm and a maximum spatial frequency of  $\nu_{max} = 769$  lp/mm. Comparing Figure 10 and Figure 11, a good conformity between the error prediction and measured wavefront error was found.

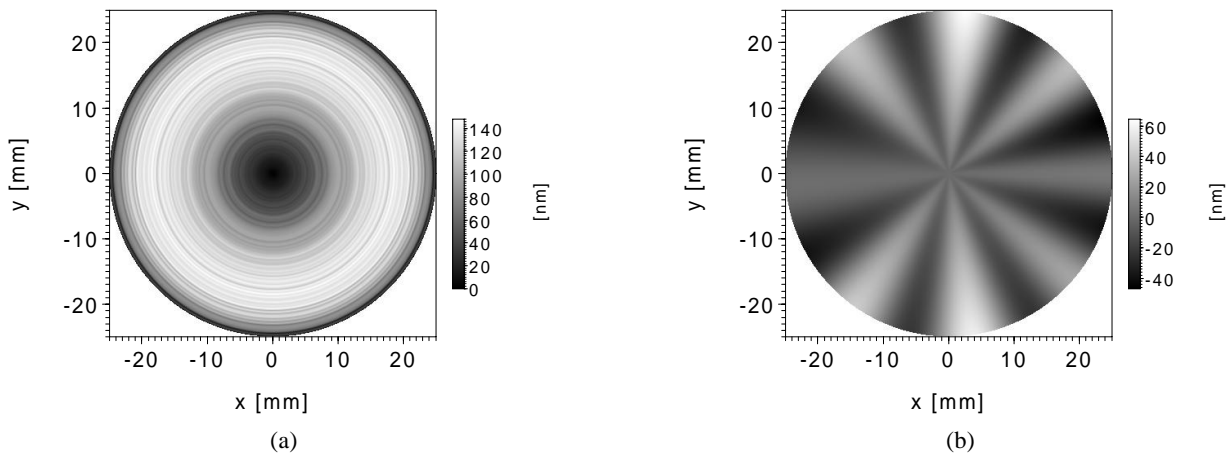


Figure 10. Prediction of the expected wavefront pattern distortion error  $W_{PD}$ , calculated from fabrication data: (a) rotationally symmetric wavefront error and (b) non-rotationally symmetric wavefront error for a  $f/1$  zone plate.

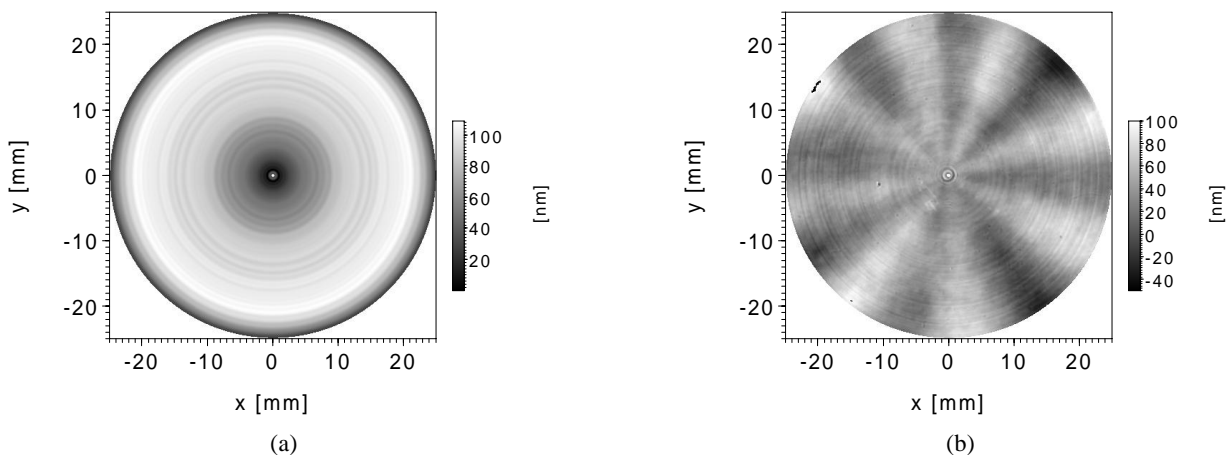


Figure 11. Wavefront error measured in a  $f/1$  Fresnel zone plate measured in reflection. Tilt and defocus are subtracted from measured data. The wavefront error is divided in (a) rotationally and (b) non-rotationally symmetric part. The observed total PV value of the wavefront error is 232 nm, the RMS value is 31 nm.

## 7. DOE FABRICATION WITH PERIODICAL CORRECTION

Correction of DOE wavefront error on the base of determined pattern error  $\zeta$  ("fabrication history") is effective only for simple optical measuring systems. In a number of cases it is necessary to guarantee the highest possible accuracy of the DOE fabrication. The method of periodical correction of the linear coordinate (see Section 4.2) can be used for that. The proposed method was tested experimentally by means of CLWS at writing of reflective zone plates (ZP) with the minimal period of rings equal to  $1.4 \mu\text{m}$  ( $f=71\text{mm}$ ,  $D=64\text{mm}$ ,  $\lambda=633\text{nm}$ ,  $\text{N.A.}=0.45$ ).

Two identical 64mm ZP were fabricated by the direct laser writing using the thermochemical technology in chromium films 70 nm thick, which were coated on high-quality fused-silica substrates. Writing time of such ZP with multi-pass writing algorithm described in section 5 was about 140 minutes. The period for correction was chosen every 3-mm (less than 18-min. of writing) since expected original coordinate drift was about 100nm/hour. Thus there were 9 points of correction at 6, 9, 12, 15, 18, 21, 24, 27 and 30-mm radii. In these points writing process was interrupted. The writing head was moved to the origin of radial coordinate for starting the center searching and radial coordinate correction. Figure 12 depicts wavefront phase error of two manufactured ZP predicted on the base of coordinate origin measurements in the points of corrections. One can see that periodical correction introduces the high frequency errors in wavefront function but very effectively decreases the center drift (see for compare with Figure 9).

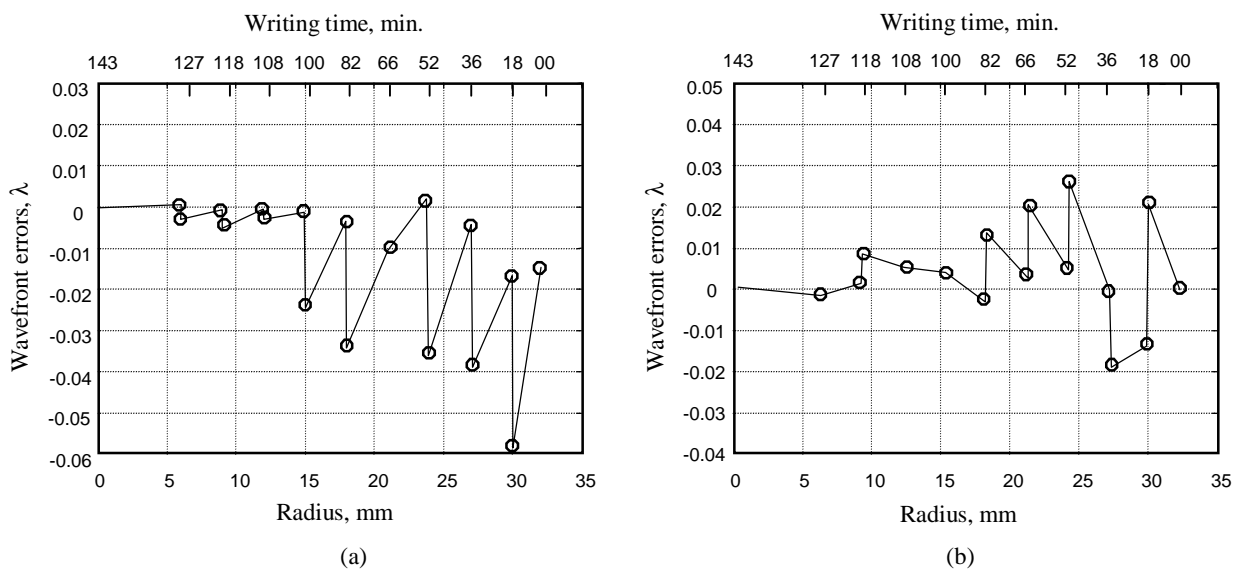


Figure 12. Wavefront phase errors of manufactured DOEs (ZP with  $f=71\text{mm}$ ,  $D=64\text{mm}$ ) predicted on the base of coordinate errors in the time of writing. a – sample # 03; b –sample #4. Circles depict the places of the coordinate correction. Left plot - sample #03 (environment:  $t=+23.5 \text{ }^\circ\text{C}$ ;  $P=991\text{mbar}$ ). Right plot - sample #04 (environment:  $t=+21.9 \text{ }^\circ\text{C}$ ;  $P=1000 \text{ mbar}$ ).

Manufactured zone plates were investigated further as reflective elements by means of a phase shift Fizeau interferometer. Figure 13 shows continuous-tone images (phase maps) of the ZP wavefront phase (a, b) and their cross-sections (c, d). The shape of diffracted wavefronts has the rms deviation from the calculated (spherical) ones equal to  $W_{rms} = 0.008$  (sample #3) and 0,009 (sample #4). It is seen that predicted (Figure 12) and measured (Figure 13) wavefronts are about the same. Thus, we can state that the method based on periodical correction allows one to improve the accuracy of the CLWS.

## 8. CONCLUSIONS

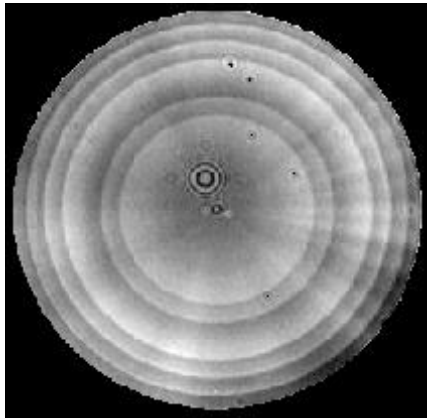
The CLWS is a high-precision system for fabrication of DOEs: gratings, zone plates, computer-generated holograms, optical limbs, etc. The accuracy, spatial resolution, and working field of CLWS are sufficient to solve a wide spectrum of problems in optics, measuring engineering, and laser technology.

Unlike the conventional systems operating in the X-Y coordinate system, CLWS has some specific sources of the writing errors that affect the quality of DOEs fabricated. They are an error in fixing the origin of coordinates, angular coordinate

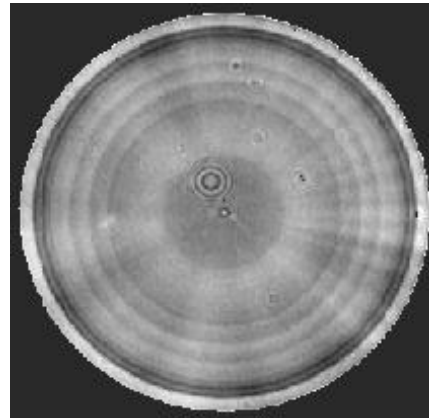
error, and imperfect rotation of the table with a substrate. It has been shown that the writing errors have influence on the quality of a DOE wavefront, the greatest effect being observed in the drift of the origin of coordinates.

Correct choice of writing strategy allows to take into consideration (Section 6) or minimize (Section 7) influence of writing errors. The axisymmetric ZPs are most suitable for testing the radial coordinate errors and the errors of fixing the origin of coordinates. Experimental investigation of the wavefronts of a ZP with 64 mm diameter and a numerical aperture of 0.45 fabricated with periodical correction has shown that the rms error does not exceed  $0.009\lambda$ .

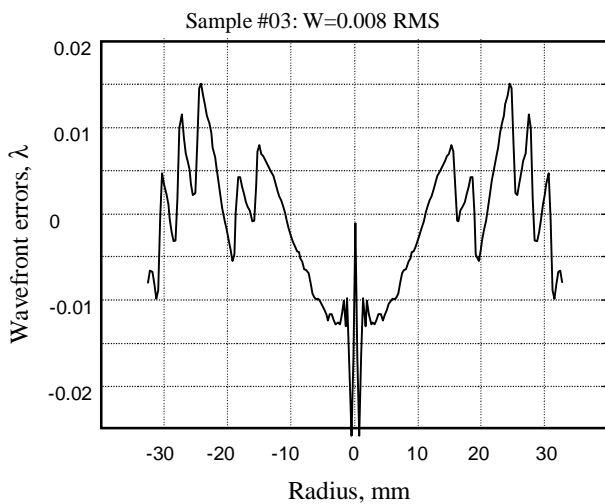
The research was partially supported by the Russian Foundation for Basis Research (grant 00-15-99089).



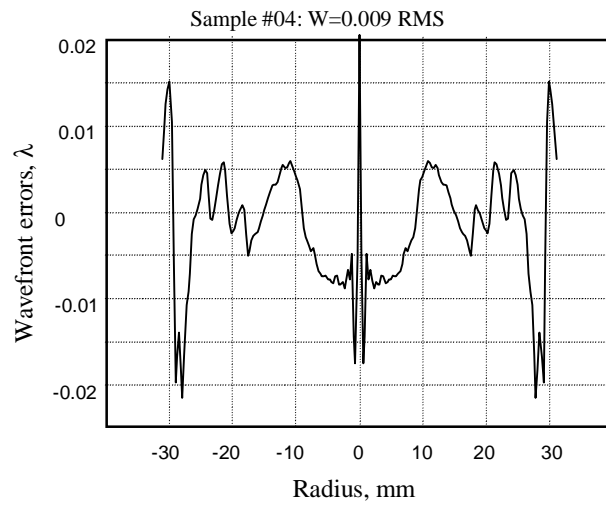
(a)



(b)



(c)



(d)

Figure 13. Measured wavefronts from 64-mm f/1 binary zone plates obtained from phase-shift Fizeau interferometer showing: (a) - gray - scale phase map that uses shading to represent phase with full scale variation  $\lambda/20$  (PV) and (b) - their cross-sections. Both samples of tested ZP show 0.008-0.009 $\lambda$  rms and 0.05 $\lambda$  PV. High frequency wavefront distortions are caused by periodical correction of the coordinate origin in the time of ZP writing.

## REFERENCES

1. J. Turunen, A. Vasara, A. Friberg, "Holographic generation of diffractive-free beams," *Appl. Optics* **27**, pp.3959-3963 (1988).

2. G. Neugebauer, R. Hauck, O. Bryngdahl, "Computer-generated holograms: carrier of polar geometry," *Appl. Optics* **24**, pp. 777-784 (1985).
3. J. H. Burge, "Applications of computer-generated holograms for interferometric measurement of large aspheric optics," in *International Conference on Optical Fabrication and Testing*, T. Kasai, SPIE **2576**, pp. 258-269 (1995).
4. J. Schwider, R. Burov. "Testing of aspherics by means of rotational-symmetric synthetic holograms," *Optica Applicata*, **VI**, 3, pp.83-88 (1976).
5. V. M. Vedernikov, V. N. Vyukhin, V.P.Koronkevich, F. I. Kokoulin, A. I. Lokhmatov, V. I. Nalivaiko, A. G. Poleshchuk, G. G. Tarasov, V. A. Khanov, A. M. Sherbachenko, and Yu. I. Yurlov, "A precision photoconstructor for synthesizing optical components," *Avtometriya*, N3, pp.3-17 (1981), (in Russian, Engl. Transl.: Optoelectronics, Instr. and Data Processing).
6. M. Haruna, M. Takahashi, K. Wakahayashi, and H. Nishihara, "Laser beam lithographed micro-Fresnel lenses," *Appl. Optics*, **29**, pp.5120-5126 (1990).
7. W. Goltsos and S. Liu, "Polar Coordinate laser writer for binary optics fabrication," in *Computer and Optically Formed Holographic Optics*, I. Cindrich and S. H. Lee, eds., SPIE **1211**, pp.137-147 (1990).
8. T. Nomura, K. Kamiya, H. Miyashiro, K. Yoshikawa, H. Tashiro, M. Suzuki, S. Ozono, F. Kobayashi, and M. Usuki, "An instrument for manufacturing zone-plates by using a lathe," *Precision Eng.* **16**, No. 4, pp.290-295 (1994).
9. J. P. Bowen, R. L. Michaels, C. G. Blough, "Generation of large-diameter diffractive elements with laser pattern generation," *Appl. Optics* **36**, pp. 8970-8975 (1997).
10. S. Ogata, M. Tada, and M. Yoneda, "Electron-beam writing system and its application to large and high-density diffractive optic elements," *Appl. Optics* **33**, pp.2032-2038 (1994).
11. A.G. Poleshchuk, E.G. Churin, V.P. Koronkevich, V.P. Korolkov, etc. "Polar coordinate laser pattern generator for fabrication of diffractive optical elements with arbitrary structure," *Appl. Opt.*, **38**, pp.1295-1301 (1999).
12. J. H. Burge. "Measurement of large convex aspheres," *Optical telescopes of Today and Tomorrow.*, SPIE **2871**, pp.362-373, (1996).
13. S. M. Arnold, R. Kestner. "Verification and certification of CGH aspheric nulls," in *Optical Manufacturing and Testing*, ed. By Victor J. Doherty; H. Philip Stahl, Proc. SPIE **2536**, pp.117-126,. (1995).
14. A. G. Poleshchuk, V. P. Koronkevich, V. P. Korolkov, A. A. Kharissov, V. V. Cherkashin, "Fabrication of diffractive optical elements in the polar coordinate system: fabrication errors and their measurement," *Avtometriya*, N6 , pp.40-53 (1997), (in Russian, Engl. Transl.: Optoelectronics, Instr. and Data Processing).
15. J.Burge, SPIE 3782. Yu-Chun Chang and James Burge. "Error analysis for CGH optical testing," *Optical Manufacturing and Testing III*, H. P. Stahl, Editor, Proc. SPIE **3782**, pp.358-366 (1999).
16. J. Guhr. "Test results of the laser writing system CLWS-300c," *Diffractive Optics' 97, Savolina, Finland. EOS Topical Meeting Digest Series: 12*, pp.206-207 (1997).
17. P. Piero, S. Sinezi, M. Ripetto, G.V. Usplenev. "Using the circular laser writing system for fabrication of DOE gray-scale masks on the base of LDW glass plates," *Computer Optics*, **17**, pp.85-93 (1997), Moscow – Samara (in Russian).
18. R. Freimann. "Aberrations of axially symmetric diffractive elements in relation to their fabrication inaccuracies," *Optik*, **111**, No. 11, pp.485-492 (2000).
19. V. P. Korolkov, R. Shimansky, A. G. Poleshchuk, V. V. Cherkashin, A. A. Kharissov, D. Denk, "Requirements and approaches to adapting laser writers for fabrication of gray-scale masks ," in *Lithographic and micromachining Techniques for Optical Component Fabrication*, SPIE **4440**, 2001.
20. V. P. Kirianov, S.A. Kokarev, "Laser - interferometric driver of displacement with subnanometer resolution," *Avtometriya*, N 2, pp.3-7 (1998).
21. V. P. Koronkevich, A. G. Poleshchuk, E. G. Churin, and Yu. Yurlov, "Selective etching of laser exposure thin chromium films," *Letters to Journal of Technical Physics* **11**, pp.144-148 (1985).
22. V. V. Cherkashin, E. G. Churin, V. P. Korolkov, V. P. Kooronkevich, A. A. Kharissov, A. G. Poleshchuk, J. H. Burge, "Processing parameters optimisation for thermochemical writing of DOEs on chromium films," in *Diffractive and Holographic Device Technologies and Applications IV*, I. Cindrich and S. H. Lee, eds., SPIE. **3010**, pp.168-179 (1997).
23. T. D. Milster, C. L. Vernold. "Technique for aligning optical and mechanical axes on a rotating linear grating," *Optical Engineering*, **34**, No. 10, pp.2840-2845 (1995).
24. W. H. Hamaker, G. Burns and P. Buch, "Optimizing the use of multipass printing to minimize printing errors in advanced laser reticle-writing systems," *15<sup>th</sup> Annual BACUS Symposium on Photomask Technology and Management*, SPIE **2621**, pp 319-328 (1995).